Microfluidic devices for studying growth and detachment of *Staphylococcus epidermidis* biofilms

Joung-Hyun Lee · Jeffrey B. Kaplan · Woo Y. Lee

Abstract Microfluidic devices were used to study the influences of hydrodynamics of local microenvironments on *Staphylococcus epidermidis* (*S. epidermidis*) biofilm formation and the effects of a poly(β-1,6-*N*-acetyl glucosamine)-hydrolyzing enzyme (dispersin B) and/or an antibiotic (rifampicin) on the detachment of the biofilm. Elongated, monolayered biofilm morphologies were observed at high flow velocity and fluid shear locations whereas large clump-like, multilayered biofilm structures were produced at low flow velocity and fluid shear locations. Upon dispersin B treatment, most of the biofilm was detached from the microchannel surface. However, a trace amount of bacterial cells could not be removed from corner locations most likely due to the insufficient wall shear stress of the fluid at these locations. Dispersin B or rifampicin treatment was effective in delaying the dispersal behavior of bacterial cells, but could not completely remove the biofilm. Combined dynamic delivery of dispersin B and rifampicin was found to be effective for complete removal of the *S. epidermidis* biofilm.

Keywords Poly(dimethylsiloxane) (PDMS) · Microfluidics · Microenvironment · *Staphylococcus epidermidis* · Dispersin B · Rifampicin · Biofilms

J.-H. Lee · W. Y. Lee (✉)
New Jersey Center for MicroChemical Systems,
Department of Chemical, Biomedical and Materials Engineering,
Stevens Institute of Technology,
Hoboken, NJ 07030, USA
e-mail: wlee@stevens.edu

J. B. Kaplan
Department of Oral Biology, New Jersey Dental School,
Newark, NJ 07103, USA

1 Introduction

There has been a rapidly growing interest to design, develop, and use microfluidic devices that can emulate biological phenomena occurring under various geometrical, fluid dynamic, and mass transport constraints of physiological microenvironments (Chen et al. 1997; Griffith et al. 2004; Huh et al. 2004; Raty et al. 2004; Atencia and Beebe 2005; El-Ali et al. 2006; Whitesides 2006). Soft lithography, based on poly(dimethylsiloxane) (PDMS), provides a simple yet versatile way of fabricating microfluidic devices with attractive properties of PDMS as a biocompatible, transparent, and elastomeric material. While most microfluidic research efforts to date have concentrated on eukaryotic cell biology (Takayama et al. 1999; Khademhosseini et al. 2004; Raty et al. 2004; Hung et al. 2005; Futai et al. 2006; Leclerc et al. 2006), microfluidics are expected to play several significant roles in advancing microbiology by precisely controlling local microenvironments surrounding microbial cells, by isolating and studying individual or small group of cells, and by providing identical and reproducible culture conditions and therefore generating quantitative data (Weibel et al. 2007).

Our long-term motivation for the present study was to explore the potential of microfluidic devices as new tools for developing predictable *in vitro* models of biofilm-related infections. In many infections, bacteria attach to the surfaces of medical devices or compromised tissue and subsequently develop into highly cooperative communities known as biofilms. Bacteria in biofilm microenvironments are well protected from host defenses and antibiotics. Biofilm infections are thus difficult to treat with conventional antibiotics, almost all of which have been developed to combat bacteria in their planktonic state. Therefore, this public health problem requires multifaceted approaches

ranging from developing biomaterials that can prevent bacterial adhesion (Furno et al. 2004; Zhao and Liu 2006; Li et al. 2007) to exploring entirely new therapeutic concepts (Reddy and Ross 2001; Harris and Richards 2006; Donelli et al. 2007).

As an example of the latter approach, Kaplan et al. have recently discovered that an enzyme, dispersin B, degrades *N*-acetylglucosamine-containing extracellular polysaccharide (EPS) and therefore provides an effective mechanism for releasing and detaching bacterial cells from *Staphylococcus epidermidis* biofilms grown attached to plastics (Kaplan et al. 2003; Kaplan et al. 2004a; Kaplan et al. 2004b; Ramasubbu et al. 2005). This discovery is important since *S. epidermidis* is a primary cause of infections of many biomedical devices such as intravascular catheters and prosthetic joints (Jupiter et al. 1981; Peters et al. 1981; Marrie and Costerton 1984; Sattler et al. 1984; Widmer 2001; Zimmerli et al. 2004; Zimmerli 2006).

For the present study, we have selected dynamic delivery of dispersin B on the detachment of *S. epidermidis* bacterial cells as an initial working example for applying microfluidic tool concepts to biofilm studies. Specifically, we designed, fabricated, and used two simple microfluidic devices to correlate biofilm formation and its detachment by the action of dispersin B with spatially resolved flow patterns and wall shear stress, and to assess potential synergy of combining dispersin B and antibiotic deliveries.

2 Experimental

2.1 *S. epidermidis* inoculum preparation

S. epidermidis strain NJ9709 (Kaplan et al. 2004a), which was isolated from the surface of infected intravenous catheter, was employed. Inoculum preparation followed the procedure described previously (Kaplan et al. 2004a) with slight modifications. In brief, a loopful of colonies scraped from the surface of an agar plate was transferred and dispersed into a tube containing 200 μl of fresh Trypticase soy broth supplemented with 6 g of yeast extract and 8 g of glucose per liter (TSB medium). The tube was vortexed for 30 s, and the cells were allowed to settle for 5 min. 100 μl of the upper layer was transferred to a polystyrene Petri dish containing 20 ml of the fresh TSB medium, and the dish was incubated overnight at 37°C. The biofilm that formed on the surface of the dish was rinsed twice with PBS and then scraped from the surface into 3 ml of TSB medium by using a cell scraper. The cell aggregate was transferred to a conical centrifuge tube, vortexed, sonicated for 30 s, and allowed to settle on the bottom of the tube for 10 min. A 0.5-ml aliquot of the top layer was transferred to a tube containing 5 ml of the fresh TSB medium, and the cells were then filtered through a 5 μm syringe filter to produce a single-cell suspension as previously described (Kaplan and Fine 2002). The concentration of the inoculum was confirmed to be approximately 1×10^9 colony forming unit (CFU)/ml by plating serial decimal dilutions of the inoculum onto 5% sheep blood agar plates and incubating overnight. This original inoculum was used for device I (Fig. 1) and further diluted to be 1×10^7 CFU/ml for device II (Fig. 2).

2.2 Enzyme and antibiotic preparation

Dispersin B, which hydrolyzes the 1→6 glycosidic bond of β-substituted *N*-acetylglucosamine, was prepared as previously described (Kaplan et al. 2004b; Ramasubbu et al. 2005). The purified enzyme had a specific activity of 970 IU per mg of the protein, where 1 IU of the enzyme activity was defined as the amount of the enzyme needed to hydrolyze 1 μmol of 4-nitrophenyl-β-D-*N*-acetylglucosaminide to 4-nitrophenol and *N*-acetylglucosamine per min at pH 4.5 at 25°C in 50 mM sodium phosphate buffer with 100 mM NaCl. Enzyme concentration for this experiment was 20 μg/ml in PBS (phosphate buffered saline). Rifampicin (Sigma Chemical Company) is a frequently used antibiotic for killing staphylococcal cells in biofilms (Zheng and Stewart 2002; Saginur et al. 2006). Rifampicin was used at a concentration of 50 μg/ml in PBS.

Fig. 1 Schematic diagram of the experimental set-up with device I. A photograph of device I (*top right*) and schematic drawings of the top and side views of the device were shown (*S. epi*, *S. epidermidis*; DspB, dispersin B; TSB, trypticase soy broth; and PBS, phosphate buffered saline)
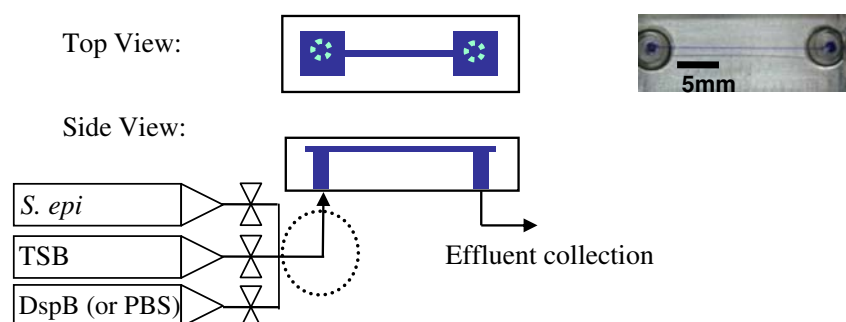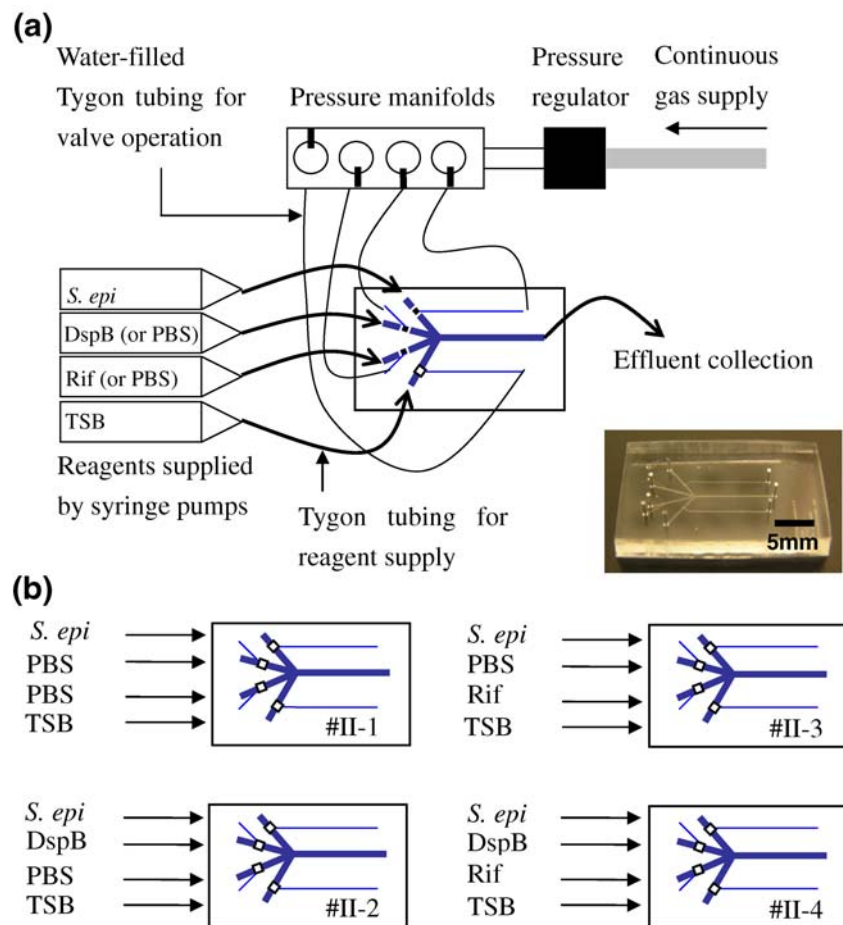
2.3 Microfluidic device design and fabrication

Schematic design features of two microfluidic devices used in this study are shown in Figs. 1 and 2. Device I (Fig. 1) was composed of a single channel (22-mm long, 100-μm width, and 100-μm depth) along with relatively large inlet or outlet areas (2×2 mm with 100-μm depth). The volume of the channel was 0.22 μl. With device I, the inoculum, culture medium, dispersin B, PBS, staining, or washing streams shared an external mixer that fed the streams into the device microchannel. It was a simple device useful for the initial biofilm growth and detachment experiments.

Device II (Fig. 2) consisted of a main channel and four inlet channels that were merged into the main channel. The width and depth of the channels were 200 and 30 μm, respectively. The volume of the main channel was 0.06 μl for device II. This device was designed with embedded micromechanical valves to: (1) avoid reagent mixing outside the device and reduce sources for cross-contamination before each stream enters into the main microchannel and (2) facilitate time-controlled and spatially confined administration of therapeutic reagents without cross-contamination between them.

Soft lithography (Takayama et al. 1999; Whitesides 2006; Weibel et al. 2007) was used to fabricate the microfluidic devices. In this method, a negative PDMS relief of microchannels was formed by curing a mixture of a base prepolymer and its curing agent (Sylgard 184, Dow-Corning) on a silicon mold surface which was patterned by photolithography with a positive relief of the channels made of a photoresist material. The patterned PDMS piece was then peeled off from the mold after curing. For the present work, several silicon molds were used to produce various patterned PDMS pieces needed to assemble the devices shown in Figs. 1 and 2. For fluidic connections, holes were created by punching at inlet and outlet of the patterned PDMS pieces. Subsequently, the patterned PDMS pieces were sealed with unpatterned PDMS or glass pieces to complete the formation of fluidic channels. Prior to the sealing step, the PDMS pieces were cleaned and activated for bonding using the following steps: (1) soft brushing with neutral soap, (2) rinsing with DI water and then ethanol, (3) drying with compressed nitrogen, and (4) plasma pretreatment at 1 kV with 300 mTorr of oxygen for 1 min. Details of micromechanical valve fabrication and pressure-activated actuation mechanisms used for device II

were described elsewhere. (Unger et al. 2000; Melin and Quake 2007).

Aluminum frames were used to hold the PDMS devices. A heating pad (HK5160, Minco) was attached to the aluminum frame to keep the temperature of the devices at 37°C. The temperature of the PDMS device surface was measured using a J type thermocouple. (TC40JT36B from Minco) All fluidic connection parts for device I (tubing 1511, connecters P-632, fittings P-235, ferrules P-200N, shut-off valves P-732, and luer adapters P-624 from Upchurch Scientific) and for device II (Tygon tubing A06418-02 from Cole-Parmer, dispensing needles 75165A684 and metal tubes NE-1300-01 from New England Small Tube) are biocompatible and were autoclaved. Syringe pumps (Kds200, KD Scientific) were used to control flow rates in the range of 5 to 30 μl/min. All the parts to be exposed to the working flow streams were autoclaved and assembled in sterile conditions.

2.4 Dynamic inoculation, culture, dispersin B and antibiotic administration

Device I was used to study the effect of dispersin B on biofilm detachment while spatially resolving local hydrodynamics with the aid of microscopy and computational flow modeling. For a set of experiment associated with device I, two devices were used for comparing dispersin B treatment to PBS treatment as a control. Each device was preconditioned with the TSB medium for 3 h and inoculated with the 1×10^9 CFU/ml S. epidermidis inoculum at a flow rate of 5 μl/min for 30 min, and were allowed to stand without flow by closing the inlet valves for 1 h. After this inoculation step, the fresh TSB medium flow was established at a flow rate of 10 μl/min to begin the culture step. After 18 h into the culture step, dispersin B was administrated into one device (device I-1) at a flow rate of 5 μl/min for 1 h. During the same time period, device I-2 was treated with 5 μl/min of PBS. Effluents exiting both the devices were collected at various time intervals to measure the number of released S. epidermidis cells in each effluent stream by plating them on the agar plates. Enzyme flow of device I-1 was replaced with the PBS flow for 1 h. This step was followed by staining biofilms formed in the devices with Gram's crystal violet (Fisher Scientific) and rinsing with sterile water.

Device II was used to investigate the effects of combined delivery of dispersin B and antibiotic under dynamic flow conditions as shown in Fig. 2. Four inlet flow channels of device II were connected with four syringes, by Tygon tubing and 23 gauge metal tubes, as shown in Fig. 2(a). Effluent collecting tubes were irrigated from one outlet flow channel of each device, and collected for every 15 min to count released bacterial cells from the device as a function of time. Each of four embedded microvalves was operated individually by pressure supplied by compressed air. Four valve control channels were connected with Tygon tubes filled with water and the tubes were connected to pressure-manifolds which regulated air pressure at 0.07–0.09 MPa. When a manifold is open, the pressure was supplied to the water. The pressurized water then collapsed an embedded microvalve membrane, resulting in the closure of the flow channel adjacent to the control channel (Unger et al. 2000; Melin and Quake 2007).

For the experiment associated with device II, four devices were run at the same time using the experimental set up and conditions schematically described in Fig. 2(a) and (b). All the devices were preconditioned overnight at a flow rate of 30 μl/min of the TSB culture medium by opening the microvalve for the fourth inlet channel. The TSB effluent was collected three times before inoculation and analyzed by the plating method during this preconditioning step to confirm the sterility of the whole experimental apparatus. Then, the devices were inoculated with S. epidermidis of 1×10^7 CFU/ml at a flow rate of 30 μl/min for 1 h by opening the valve for the first inlet channel while closing the other valves. The effluents from each device were collected for every 15 min for the plating. At the end of the inoculation step, all valves were closed and the fluid captured in the main microchannel was allowed to stand for 10 min. The culture step was initiated by re-establishing the TSB medium flow at a flow rate of 30 μl/min by opening the valve for the fourth inlet channel and was continued for overnight in order for S. epidermidis biofilm to grow inside the main microchannel.

Dispersin B and antibiotic administrations were conducted at 24 h from the beginning of the inoculation step for the device II experiments using the microvalves for the second and third inlet channels. Device II-1 was treated with PBS as a control. Device II-2 and II-3 were treated with dispersin B and rifampicin, respectively, at a flow rate of 30 μl/min for 1 h. Device II-4 was treated with dispersin B for 30 min, and then with rifampicin for another 30 min while keeping the same flow rate of 30 μl/min. During the reagent treatments, the TBS flow through the fourth inlet was stopped. Flows through the four inlets were not mixed, but were made sequentially, so that only one valve was open for flow at a time while the other valves were kept closed. After these treatments, the culture step was re-established and continued for 5 days. During the 5-day culture period, the effluent from each device was collected and plated at every 15 min to measure the release of planktonic bacterial cells from each device. At the end of the culture step, the devices were washed with PBS and then stained with crystal violet and rinsed with sterile water.

2.5 Imaging of biofilm formed on microchannels

After the culture experiments, distributions of *S. epidermidis* colonies formed on various microchannel locations from the device I were imaged with a Nikon eclipse E1000 light microscope fitted with a SensiCam high performance camera (Cooke Corporation). Also, a LEO 982 Scanning electron microscope (SEM) with a field emission gun was used to image bacteria cells at an accelerating voltage of 1 kV. Samples for the SEM analysis were fixed with 4% paraformaldehyde in PBS for 10 min, followed by dehydration in a series of diluted ethanol.

2.6 Computational fluid dynamics simulation

The flow behavior inside device I was analyzed using a computational fluid dynamic (CFD) software package FLUENT (version 6.2.16, Fluent Inc., Lebanon, NH, USA). A pre-processor software in the package, GAMBIT, (version 2.2.30, Fluent Inc., Lebanon, NH, USA) first created the geometry and then meshed it. A non-uniform hexahedral grid was used in the simulation. After the program was converged, all the flow parameters such as velocity and pressure fields were obtained, and these data together with all other derivative data such as wall shear stress were stored in the data file. A post-processor generated 2D x–y plots as well as 3D contour and velocity field plots. The velocity profile, pressure drop and wall shear stress were estimated assuming the water flow rate of 1 µl/min and the physical properties of pure water.

3 Results and discussion

3.1 Effects of local hydrodynamics on biofilm formation

Figure 3 shows microscopic images of *S. epidermidis* biofilm formed in device I-2. Populations and morphologies of the biofilm grown were different depending on microchannel locations. Large clump-like, multilayered structures were found at the inlet and outlet parts of the device [Fig. 3 (a–d)]. SEM images showed that extracellular polysaccharide matrix surrounded individual cells [Fig. 3(c, d)]. On the other hand, mostly monolayered structures and at some locations bilayered structures were found along the main microchannel with much less apparent appearance of the polysaccharide matrix [Fig. 3 (e–h)].

For the TSB medium flow rate of 10 µl/min, the Reynolds numbers were estimated to be about 1.9 and 3.6 at the channel and inlet/outlet regions, respectively, of device I. At these very low Reynolds numbers, the flow at the both regions was expected to be highly laminar, which

is a well known characteristic for microfluidics (Stoodley et al. 1999; Stoodley et al. 2002; Hall-Stoodley et al. 2004; Alejandro Bonilla et al. 2007). Note that the flow patterns in the outlet region were similar to those in the inlet region except for the direction of velocity vectors. As shown in Fig. 4, wall shear stress contours and velocity profiles are compared for the microchannel and inlet regions. For example, the average magnitude of the velocity vectors was estimated to be about 1 mm/s near the bottom wall of the microchannel while that near the top wall of the inlet region was as low as about 10^{-6} mm/s (i.e., virtually stagnant). The hydrodynamic velocity was substantially higher in the microchannel region basically because of the small cross-section area to the flow and the absence of stagnant regions. The wall shear stress was calculated to be about 0.15 Pa at the middle portion of the microchannel wall, about 0.04 Pa at the corner location of the microchannel, and about 0.01 Pa at the top wall of the inlet region.

The computational fluid dynamic (CFD) estimations showed that hydrodynamic microenvironments significantly varied within device I. Our result suggested that the morphology of *S. epidermidis* biofilm formation was consequently affected by the hydrodynamics of local microenvironments. Cells arrived and adhered on the microchannel wall were exposed to the relatively fast moving fluid and high wall shear stress. The high wall shear stress conditions could limit vertical biofilm growth, resulting in the observed monolayered structure. High wall shear stress could also promote lateral growth, especially along the direction of flow as evident from Fig. 3(e) and (f). On the other hand, cells in the stagnant areas of the inlet and outlet regions were able to divide and proliferate more freely, resulting in the formation of a large multilayered structure. Our observations were somewhat consistent with the previously known effects of hydrodynamics on biofilm morphology (Dunsmore et al. 2002; Stoodley et al. 2002). They observed that biofilms of both *Pseudomonas* and sulphate-reducing *Desulfovibrio* grown under high shear were elongated along the flow direction and formed filamentous streamers whereas those grown under low shear consisted of hemispherical isotropic mound-shaped colonies.

3.2 Effects of dynamic dispersin B delivery on biofilm detachment

The effects of the dynamic dispersin B treatment on *S. epidermidis* biofilm observed in Devices I-1 and I-2 are summarized in Fig. 5. As described in the experimental section, device I-1 was treated with dispersin B after growing the *S. epidermidis* biofilm for 18 h [Fig. 5(b)] whereas device I-2 was treated with PBS as a control

Fig. 3 *S. epidermidis* biofilm formation in device I-2 at: inlet regions (**a**–**d**) and microchannel (**e**–**h**). (**a**) and (**e**) are optical microscopic images, and the others are SEM images
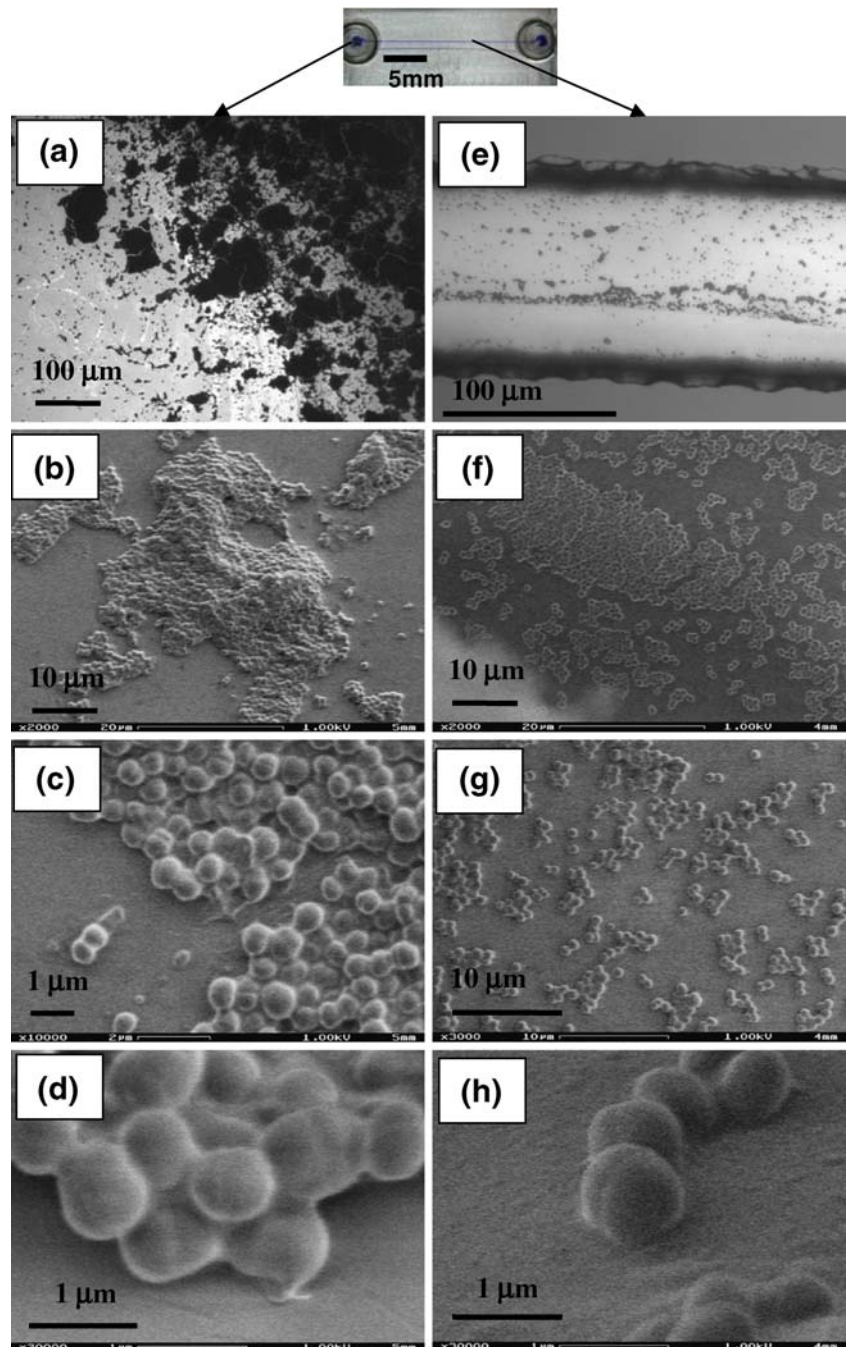
[Fig. 5(a)]. It was apparent from these microscopic images that the biofilm was mostly removed from the channel surface after the dispersin B treatment. However, there were some undetached bacterial cells left in corner locations of the microchannel [Fig. 5(c)].

Detachment of the *S. epidermidis* biofilm by the treatment of dispersin B under dynamic flow conditions can be divided into two steps: (1) enzymatic hydrolysis of the polysaccharide matrix by dispersin B (Kaplan et al. 2004b; Chaignon et al. 2007) and (2) physical removal of

individual bacterial cells and hydrolyzed matrix residues from the PDMS surfaces by fluidic shear stress. In that regard, mass transfer of the enzyme to the walls (top, bottom, or either side walls) of the device #I-1 occurred, since the enzymatic hydrolysis of EPS was evident from comparing Fig. 5(a) and (b). The shear stress at the middle part of the microchannel was estimated to be about 0.15 Pa whereas that at the corner location was much lower (about 0.04 Pa) due to the development of flow stagnation at the corner location as illustrated in Figs. 5(d) and 4. Our

Fig. 4 Shear stress contours and velocity vector profiles for device I at the average water flow rate of 1 μl/min: (**a**) wall shear stress contours at the top wall of the inlet area, (**b**) shear stress contours at the cross-section of the microchannel, (**c**) velocity vector profiles of the inlet area, and (**d**) velocity vector profiles along the microchannel
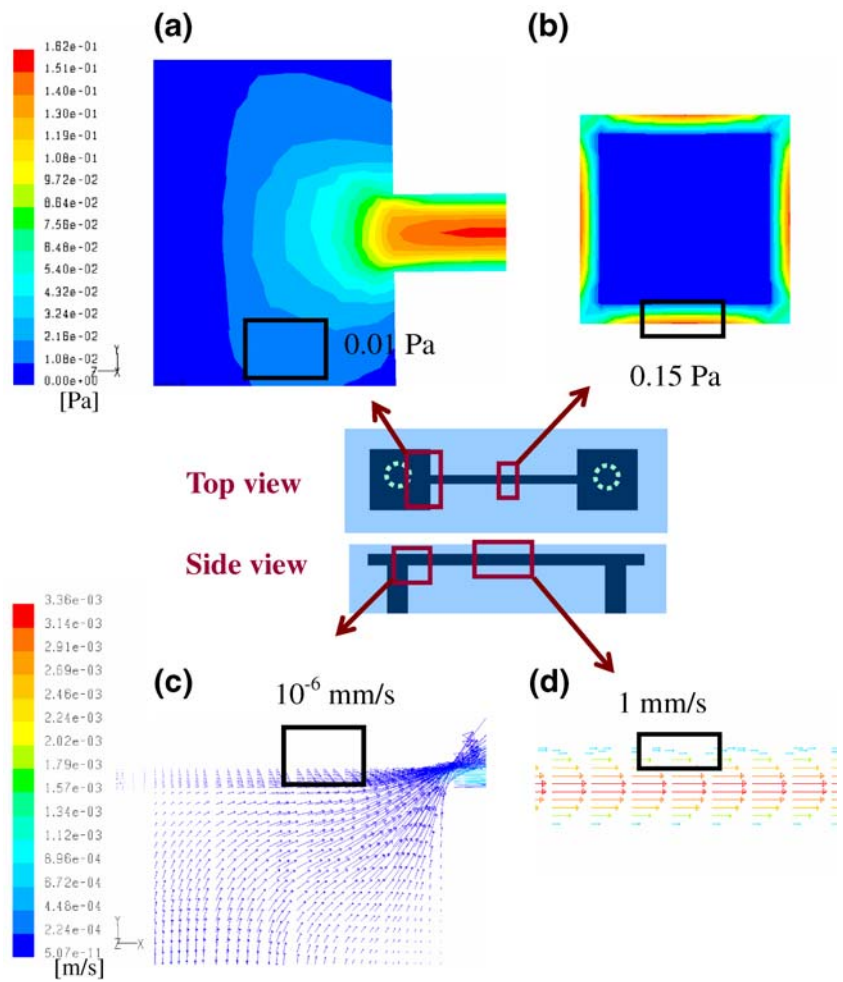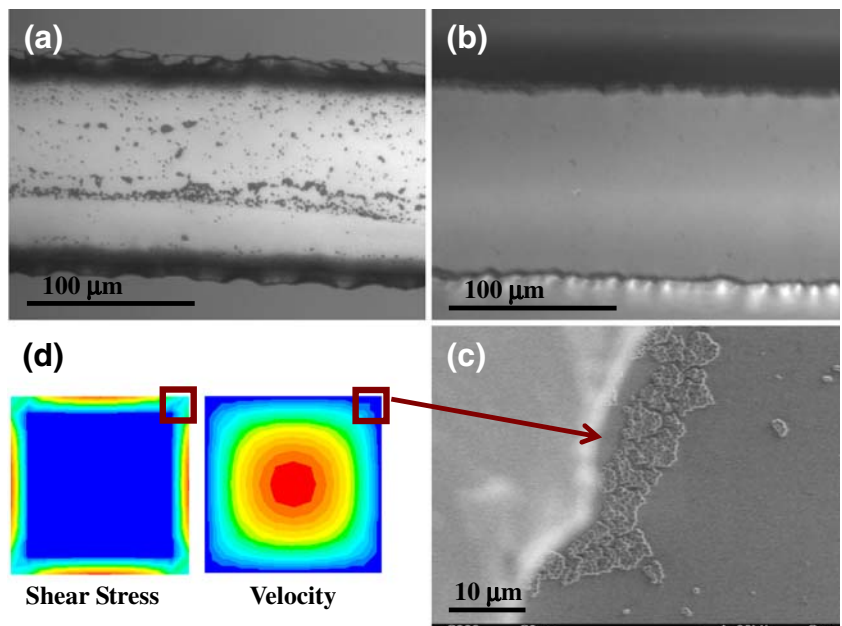

Fig. 5 Optical and scanning electron microscopic images: (**a**) device I-2 (PBS treated), (**b**) and (**c**) device I-1 treated with dispersin B, and (**d**) shear stress and velocity contours at the cross-section of the microchannel
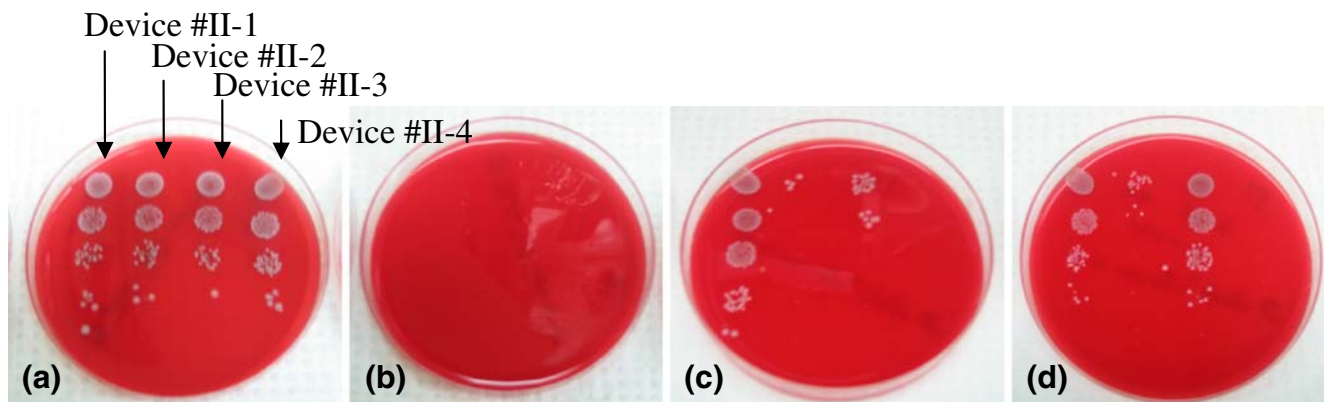
Fig. 6 The experiment with Device II was performed in five distinct stages: (1) preconditioning in TSB overnight, (2) inoculation for 1 h, (3) culture in TSB for 23 h, (4) treatment with dispersin B and/or antibiotic or PBS for 1 h, and (5) culture in TSB for 5 days. This figure shows effluent plating data obtained from Devices II-1 through II-4 at several different time points: (a) during the inoculation step, (b) 1 h after the inoculation step, (c) 24 h after the treatment step, and (d) 55 h after the treatment step. Device II-1 was treated with PBS, device II-2 and II-3 were treated with dispersin B and rifampicin, respectively, and device II-4 was treated both dispersin B and rifampicin. Top rows of each plate are for ten time dilutions of the effluents as labeled with further decimal dilutions continued below for each effluent

observations seem to suggest that the undetached biofilm left in the corner location of the mid-channel might be explained by the insufficient wall shear stress of the fluid.

3.3 Effects of combined delivery of dispersin B and antibiotic on biofilm detachment

Figure 6 shows some of the effluent plating results obtained at several experimental stages from the four devices used for the dispersin B and antibiotic delivery experiments shown in Fig. 2. Each plating spot was developed from 5 μl of one tenth of effluent or its serial decimal dilution, thus the inoculum concentration of each device was confirmed to be about 10^7 CFU/ml TSB by collecting and plating the inoculum passed through the four devices during the inoculation step [Fig. 6(a)]. Planktonic cells did not exit the devices at 1 h after the inoculation step, as they were not detected by the plating method [Fig. 6(b)]. At 24 h after the treatment step, distinctively different bacterial dispersal behavior was observed for each device [Fig. 6(c)]. Dispersal was about 4×10^7 CFU/ml, 1×10^4 CFU/ml, and 2×10^5 CFU/ml, from Devices II-1 (treated with PBS), II-2 (treated with dispersin B only) and II-3 (treated with rifampicin only), respectively. No dispersal was observed from device II-4 (treated with both dispersin B and rifampicin). At 55 h after the treatment step [Fig. 6(d)], device II-3 released approximately the same number of cells as with device II-1 (1×10^7 CFU/ml), suggesting that the antibiotic treatment became no longer effective. Also, at this time, device II-2 released significantly less cells (6×10^4 CFU/ml), while device II-4 produced no dispersal.

Figure 7 plots the number of cells released from Devices II-1 through II-4 as a function of accumulative culture time measured from the beginning of the 1-h inoculation step.

The number of released bacterial cells was measured by plating and counting colonies from effluent collected from each device as shown in Fig. 6. The detection of a significant number of released cells can be interpreted as the development of mature biofilms which disperse their planktonic cells. By 24 h from the beginning of inoculation step, very few bacterial cells were released from the devices. During this adhesion and colony forming period, the inoculated bacteria appeared to actively adhere on and colonize the PDMS microchannel surface. At 25 h after inoculation, the released cell number for the control device (i.e., PBS treatment) began to increase sharply and reached the inoculum concentration by about 30 h, and stayed at the
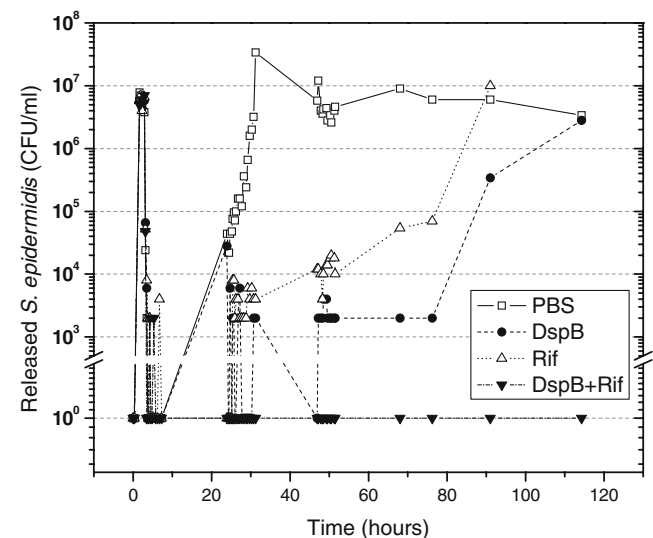

Fig. 7 Number of released *S. epidermidis* cells as a function of accumulative culture time for the labeled treatments. The accumulative culture time was measured from the beginning of the 1-h inoculation step. The treatments were performed after 24 h from the beginning of the inoculation step for the period of 1 h

level up to 120 h. In reference to the control device, the dispersin B-treated and rifampicin-treated devices showed delayed dispersal behavior. The delay caused by dispersin B was longer than that by rifampicin. The results indicated that *S. epidermidis* biofilm may persist after antibiotic or dispersin B treatment in the microfluidic conditions. In contrast, the device with the combined delivery of dispersin B and rifampicin exhibited no bacterial dispersal until the end of this experiment. The results suggest that the combined delivery of dispersin B and rifampicin is synergistic and warrant further investigations. A possible explanation for the synergy would be that dispersin B hydrolyzed extracellular polysaccharide into monosaccharides so that individual bacterial cells were no longer protected by the polymer matrix. Under this situation, the antibiotic may be able to attack and kill all bacterial cells (Donelli et al. 2007).

3.4 Considerations for device improvements

The results in the above sections clearly show the potential of using microfluidic devices with embedded microvalves for screening the effects of therapeutic reagents and strategies on biofilm study under spatially and temporary resolved dynamic microenvironments. One issue with current device design is that PDMS is not a commonly used material for biomedical implants, although its primary chemical structure and material properties are similar to those of silicones used for indwelling biomedical devices such as catheters, drains, and shunts (Ratner et al. 2004). Therefore, biofilms that are formed on actual implant surfaces may not respond exactly the same way to the treatments described in this article. In this regard, the clinical relevance of microfluidic devices can be further improved if we can incorporate an actual implant material surface as a part of microfluidic device fabrication and develop an ability to directly monitor cell-material interactions using *in-situ* imaging techniques. These improvements will considerably increase the complexity of device design and fabrication procedures, but can certainly be made. Our current effort is focused on these aspects of device improvements.

4 Conclusions

We have made our first step to explore the potential of microfluidic devices as new tools for developing predictable *in vitro* models of biofilm-related infections. We have selected dynamic delivery of dispersin B on the detachment of *S. epidermidis* bacterial cells as an initial working example for applying microfluidic tool concepts to biofilm studies. Two types of PDMS microfluidic devices were designed, fabricated, and used for studying *S. epidermidis* biofilm formation and the effect of poly(β-1,6-*N*-acetyl glucosamine)-hydrolyzing dispersin B on the detachment of the biofilm under dynamic microenvironments. The biofilm growth and its morphology were strongly affected by the hydrodynamics of local microenvironments. Elongated, monolayered biofilm morphologies were observed at high flow velocity and fluid shear locations whereas large clump-like, multilayered biofilm structures were produced at low flow velocity and fluid shear locations of the same microfluidic device. Upon dispersin B treatment, most of the biofilm was detached from the microchannel surface. However, a trace amount of bacterial cells could not be removed from stagnant or corner locations of the device most likely due to the insufficient wall shear stress of the fluid at these locations. Treatment with either Dispersin B or rifampicin was effective in delaying the dispersal behavior of bacterial cells, but was not effective in eradicating the biofilm completely. The combined dynamic delivery of dispersin B and rifampicin was observed to be effective in eradicating the *S. epidermidis* biofilm formed in the microfluidic device.

References

F. Alejandro Bonilla, N. Kleinfelter, J.H. Cushman, Adv. Water Resour **30**, 1680–1695 (2007)

J. Atencia, D.J. Beebe, Nature **437**, 648–655 (2005)

P. Chaignon, I. Sadovskaya, C. Ragunah, N. Ramasubbu, J.B. Kaplan, S. Jabbouri, Appl. Microbiol. Biotechnol. **75**, 125–132 (2007)

C.S. Chen, M. Mrksich, S. Huang, G.M. Whitesides, D.E. Ingber, Science **276**, 1425–1428 (1997)

G. Donelli, I. Francolini, D. Romoli, E. Guaglianone, A. Piozzi, C. Ragunath, J.B. Kaplan, Antimicrob. Agents Chemother **51**, 2733–2740 (2007)

B.C. Dunsmore, A. Jacobsen, L. Hall-Stoodley, C.J. Bass, H.M. Lappin-Scott, P. Stoodley, J. Ind. Microbiol. Biotech **29**, 347–353 (2002)

J. El-Ali, P.K. Sorger, K.F. Jensen, Nature **442**, 403–411 (2006)

F. Furno, K.S. Morley, B. Wong, B.L. Sharp, P.L. Arnold, S.M. Howdle, R. Bayston, P.D. Brown, P.D. Winship, H.J. Reid, J. Antimicrob. Chemother **54**, 1019–1024 (2004)

N. Futai, W. Gu, J.W. Song, S. Takayama, Lab on a Chip—Miniaturisation for Chemistry and Biology **6**, 149–154 (2006)

L. Griffith, K. Domansky, A. Sivaraman, N.C. Tedford, R.A. Aranout, D.B. Stolz, The 8th International Conference on Miniaturized Systems for Chemistry and Life Sciences **2**, 154–158 (2004)

L. Hall-Stoodley, J.W. Costerton, P. Stoodley, Nat. Rev. Microbiol **2**, 95–108 (2004)

L.G. Harris, R.G. Richards, Injury **37**(Suppl 2), S3–S14 (2006)

D. Huh, Y. Kamotani, J.B. Grothberg, S. Takayama, The 8th International Conference on Miniaturized Systems for Chemistry and Life Sciences **2**, 282–284 (2004)

P.J. Hung, P.J. Lee, P. Sabounchi, N. Aghdam, R. Lin, L.P. Lee, Lab on a Chip—Miniaturisation for Chemistry and Biology **5**, 44–48 (2005)

J.B. Jupiter, A.W. Karchmer, J.D. Lowell, W.H. Harris, J Bone Jt Surg A **63**, 194–200 (1981)

J.B. Kaplan, D.H. Fine, Appl. Environ. Microbiol **68**, 4943–4950 (2002)

J.B. Kaplan, M.F. Meyenhofer, D.H. Fine, J. Bacteriol **185**, 1399–1404 (2003)

J.B. Kaplan, C. Ragunath, K. Velliyagounder, D.H. Fine, N. Ramasubbu, Antimicrob. Agents Chemother **48**, 2633–2636 (2004a)

J.B. Kaplan, K. Velliyagounder, C. Ragunath, H. Rohde, D. Mack, J.K.M. Knobloch, N. Ramasubbu, J. Bacteriol **186**, 8213–8220 (2004b)

A. Khademhosseini, K.Y. Suh, J.M. Yang, G. Eng, J. Yeh, S. Levenberg, R. Langer, Biomaterials **25**, 3583–3592 (2004)

E. Leclerc, B. David, L. Griscom, B. Lepioufle, T. Fujii, P. Layrolle, C. Legallaisa, Biomaterials **27**, 586–595 (2006)

J.X. Li, J. Wang, L.R. Shen, Z.J. Xu, P. Li, G.J. Wan, N. Huang, Surf. Coat. Technol. **201**, 8155–8159 (2007)

T.J. Marrie, J.W. Costerton, J. Clin. Microbiol **19**, 687–693 (1984)

J. Melin, S.R. Quake, Annu. Rev. Biophys. Biomol. Struct **36**, 213–231 (2007)

G. Peters, R. Locci, G. Pulverer, Zentralblatt fur Bakteriologie Mikrobiologie und Hygiene—Abt. 1 Orig. B Hygiene **173**, 293–299 (1981)

N. Ramasubbu, L.M. Thomas, C. Ragunath, J.B. Kaplan, J. Mol. Biol **349**, 475–486 (2005)

B.D. Ratner, A.S. Hoffman, F.J. Schoen, J.E. Lemons, Biomaterials Science: An Introduction to Materials in Medicine, 2nd edn. (Elsevier, Amsterdam, 2004)

S. Raty, E.M. Walters, J. Davis, H. Zeringue, D.J. Beebe, S.L. Rodriguez-Zas, M.B. Wheeler, Lab on a Chip—Miniaturisation for Chemistry and Biology **4**, 186–190 (2004)

K. Reddy, J.M. Ross, Infect. Immun **69**, 3472–3475 (2001)

R. Saginur, M.S. Denis, W. Ferris, S.D. Aaron, F. Chan, C. Lee, K. Ramotar, Antimicrob. Agents Chemother. **50**, 55–61 (2006)

F.R. Sattler, J.B. Foderaro, R.C. Aber, Infect. Control **5**, 279–283 (1984)

P. Stoodley, I. Dodds, J.D. Boyle, H.M. Lappin-Scott, J. Appl. Microbiol. Symp. Suppl. **85**, 195–285 (1999)

P. Stoodley, R. Cargo, C.J. Rupp, S. Wilson, I. Klapper, J. Ind. Microbiol. Biotech **29**, 361–367 (2002)

S. Takayama, J.C. McDonald, E. Ostuni, M.N. Liang, P.J.A. Kenis, R.F. Ismagilov, G.M. Whitesides, Proc. Natl. Acad. Sci. U.S.A **96**, 5545–5548 (1999)

M.A. Unger, H.P. Chou, T. Thorsen, A. Scherer, S.R. Quake, Science **288**, 113–116 (2000)

D.B. Weibel, W.R. DiLuzio, G.M. Whitesides, Nat. Rev. Microbiol **5**, 209–218 (2007)

G.M. Whitesides, Nature **442**, 368–373 (2006)

A.F. Widmer, Clin. Infect. Dis. **33** (5 Suppl. 2) S94–S106 (2001)

Q. Zhao, Y. Liu, J. Food Eng **72**, 266–272 (2006)

Z. Zheng, P.S. Stewart, Antimicrob. Agents Chemother **46**, 900–903 (2002)

W. Zimmerli, A. Trampuz, P.E. Ochsner, N. Engl. J. Med **351**, 1645–1654 (2004)

W. Zimmerli, Best Pract Res Clin Rheumatol **20**, 1045–1063 (2006)